

Field-induced reorientation of nematic liquid crystals with twofold degenerate alignment on SiO_x surfaces

P. Jägemalm,¹ G. Barbero,² L. Komitov,¹ and A. K. Zvezdin^{2,3}

¹*Department of Microelectronics and Nanoscience, Chalmers University of Technology, 412 96 Göteborg, Sweden*

²*INFN and Dipartimento di Fisica del Politecnico di Torino, Corso Duca degli Abruzzi 24, 10129 Torino, Italy*

³*Institute of General Physics of the Russian Academy of Sciences, Vavilov Street 38, 117338 Moscow, Russia*

(Received 8 June 1998)

We show that an electric field normal to the boundaries confining a slab of nematic liquid crystals can induce a large change of the in-plane preferred orientation (i.e., the azimuthal angle). The degree of reorientation is controlled by the surfaces which have been coated with obliquely evaporated SiO_x. The experimental data are compared with simulations of a theoretical model where the effects of both large and small electric fields on the nematic orientation are considered. The reorientation phenomenon caused by the electric field appears to be a threshold phenomenon, due to the symmetry of the initial nematic orientation. For fields larger than the critical one, it is possible to define an effective surface energy for the system, containing the anisotropic surface energy and the contribution from the electric field. [S1063-651X(98)12211-0]

PACS number(s): 61.30.Gd, 78.20.Jq

I. INTRODUCTION

The surface orientation of nematic liquid crystals is due to the interaction of the liquid-crystal molecules with the substrate and to the incomplete nematic-nematic interaction [1]. Since the two kinds of interactions usually depend on the temperature in different manners, it is not surprising to find surface orientations that are temperature dependent. The phenomena in which the nematic surface orientation changes with temperature are known as *temperature-induced surface transitions* [2]. These kinds of transitions have recently been investigated by many groups, mainly for their application potential [3–7]. Of special interest is the temperature dependence of the nematic orientation on obliquely evaporated SiO_x, since these kinds of aligning layers have been suggested for bistable switching [8,9]. Devices acting on a basis of such layers take advantage of the twofold degeneracy in molecular orientation, which is a consequence of the symmetry of the evaporated surface. Thus, the switching ideally occurs between two symmetrically oriented and equally probable orientations.

In this paper we analyze a temperature-induced surface transition in a nematic liquid crystal, aligned by obliquely evaporated SiO_x, where the liquid-crystal layer is submitted to an external electric field applied across the sample. We shall show that the external field, oriented normally to the substrates, may change the temperature-induced surface transition both for the polar and the azimuthal orientation. Our paper is organized as follows: The experiment and the observed orientational transitions are described in the next section. In Sec. III A the elastic description of the nematic sample is presented. There we derive the bulk equilibrium equations and the relevant boundary conditions. We will show that in the presence of an electric field it is possible to introduce an effective anchoring energy. This effective anchoring energy takes into account the destabilizing effect due to the applied field and the stabilizing effect due to the surface forces. By means of this quantity, in Sec. III B the ac-

tual nematic orientation is determined in general. The special case in which the reorientation of the director at the SiO_x surface occurs in a plane is analyzed in Sec. III C, where the effect of large electric fields on the nematic surface orientation is discussed. The effect of an electric field close to the threshold is considered in Sec. III D. Finally, the theoretical and experimental results are compared and discussed in Sec. IV.

II. EXPERIMENT

A. Cell preparation and characterization

The liquid-crystal samples used in the experiments were of the standard sandwiched type of cells, consisting of two parallel glass plates separated at a distance of about 3 μm from each other; see Fig. 1(a). The distance between the two plates was kept constant by spacers made of evaporated SiO_x and the achieved cell thickness was calculated from interference fringes measured by a spectrophotometer. The cells were made from ITO covered glass (Baltracon Z20) with aligning layers of obliquely evaporated SiO_x [10]. The SiO_x was evaporated at 8 Å/s and to a thickness of 200 Å, measured by a quartz oscillator oriented perpendicularly to the evaporation direction. In this study the evaporation angle α (defined as the angle between the evaporation direction and the substrate normal) was kept constant at about 74°. All depositions were carried out at room temperature and in high vacuum (10⁻⁷ mbar, SiO source). In order to achieve a uniform and undeformed liquid-crystal orientation, the two plates were assembled with their evaporation directions antiparallel to each other. The filling of the cells took place under vacuum and with the liquid-crystal material in the isotropic phase. We used the material E7 (Merck) which has a nematic phase in the temperature range -30 °C to 58 °C and a positive dielectric anisotropy, $\Delta\epsilon = +13.8$ (1 kHz, 20 °C). The observations of the textures and the electrically induced surface transitions were performed using a polarizing microscope (Zeiss Photo microscope II Pol.) and with the

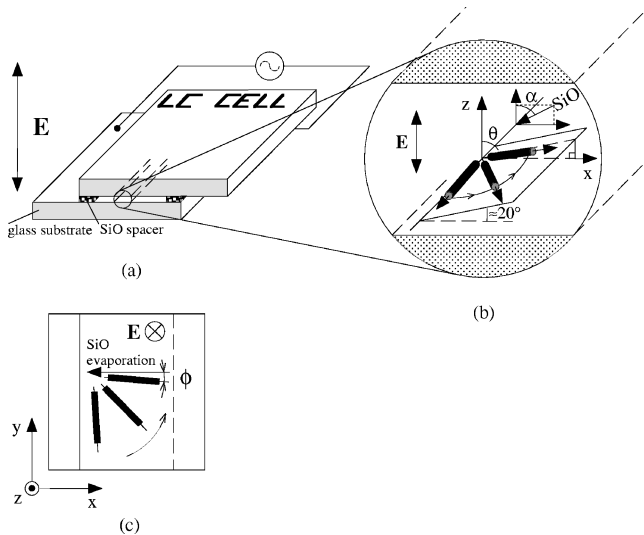


FIG. 1. Schematic sketch of the field-induced reorientation of nematic-liquid-crystal molecules on evaporated SiO_x . (a) The cell geometry. (b) The molecular reorientation process at one of the surfaces in the cell. The plane of reorientation is tilted at about 20° with respect to the substrate plane and the polar angle is indicated as θ , whereas the evaporation angle is represented by α . (c) The reorientation process as projected on the substrate plane. The azimuthal angle ϕ is measured in the plane of the sample.

liquid-crystal cell kept in a hot stage (Mettler FP52) attached to the turntable of the microscope. The hot stage controls the temperature of the cell during the observation to within $\pm 0.1^\circ\text{C}$. With crossed polarizer and analyzer, it is straightforward to determine the extinction angles and thereby the preferred orientation of the liquid-crystal layer at various temperatures and applied electric fields. The voltage was applied to the ITO electrodes on each glass substrate and thus the electric field was along the normal of the cell surfaces.

B. Orientational transitions on evaporated SiO_x

The structure of the evaporated SiO_x surface depends strongly on the evaporation angle and on the thickness of the SiO_x layer [11,12]. According to Ref. [12] this is due to a structural transition in the SiO_x , from a columnarlike to a needlelike structure. The structural change of the surface is then followed by a corresponding transition in the orientation of nematic liquid crystals in contact with the substrates. These transitions in the liquid-crystal orientation have long been studied as a function of the evaporation angle and of the SiO_x thickness [3–5,11–14].

Now, consider the geometry described in Fig. 1(b). The SiO_x evaporation direction lies in the x - z plane, which by definition also is the evaporation plane. For the liquid-crystal material E7, the orientational transition upon varying the evaporation angle α occurs in the small range from 67° to 75° [5] (the transition has been reported to be in a similar range for other nematic materials). For evaporation angles lower than 67° , the nematic orientation is perpendicular to the evaporation plane and with zero pretilt [polar angle $\theta = 90^\circ$ and azimuthal angle $\phi = 90^\circ$, where the angles are defined in Figs. 1(b) and 1(c)]. For evaporation angles larger than 75° , the orientation is instead in the evaporation plane and with a pretilt of about 20° from the substrate ($0^\circ < \theta$

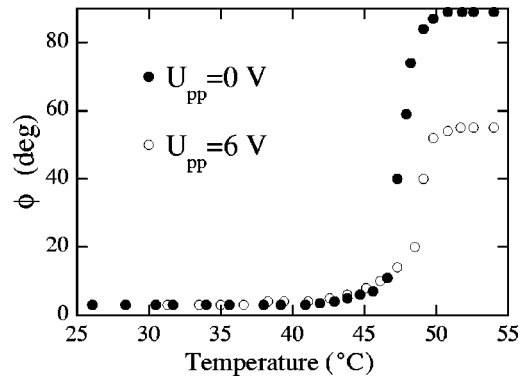


FIG. 2. The temperature-induced reorientation with and without an applied electric field (U_{pp} , ac voltage; $f = 100$ Hz). The reorientation saturates at a lower value of ϕ when the field is applied than without. This orientational transition follows the plane described for the field-induced transition in Fig. 1(b). The SiO_x evaporation angle is $\alpha = 74^\circ$, the cell gap $d = 3 \mu\text{m}$, and the liquid-crystal material is E7.

$< 90^\circ$, $\phi = 0^\circ$). By varying the evaporation angle between these two limiting values, the nematic orientation is changing continuously, but lies all the time on a *plane* which is tilted at about 20° from the substrate plane [3] and has its normal in the evaporation plane [this plane of reorientation is shown in Fig. 1(b)]. In practice, these various orientations correspond to the liquid-crystal orientation in cells made with different evaporation angles and thus cannot be seen as an orientational transition in one single location in a cell. From the symmetry of the evaporated surface, it follows that two equally probable orientations are allowed, each one making an angle ϕ and $-\phi$ with the evaporation plane, respectively. In this study, however, we concentrate on the orientations in one of these types of domains (the behavior of the other domain is similar). This type of alignment, which usually is called the twofold-degenerate tilted alignment, has already been suggested for bistable switching [8,9], as mentioned in the Introduction. It has also been used in a study with a geometry similar to ours [15], in order to study the anchoring anisotropy close to the bifurcation from a monostable to the twofold-degenerate alignment.

Recently it was shown that the orientation in the twofold-degenerate anchoring is temperature dependent [5,7]. The effect of increasing the temperature is that the orientation moves towards the position perpendicular to the evaporation plane. The initial orientation is determined by the value of the evaporation angle and is somewhere on the plane described above. Then, as the temperature is increased, the director reorients on that plane until it reaches the position perpendicular to the evaporation plane. On decreasing the temperature, the director moves back to the initial orientation, showing a small hysteresis [5]. A measurement of the azimuthal angle of the director in the temperature-induced transition is shown in Fig. 2, where the small hysteresis has been neglected (the transition is shown with and without an applied electric field). This temperature-induced transition was analyzed in Refs. [5, 16] and it was shown that the director essentially follows the same plane as upon varying the evaporation angle, as described above and reported by Monkade *et al.* [3]. In this paper, the central point is to show how this temperature-induced transition is affected by apply-

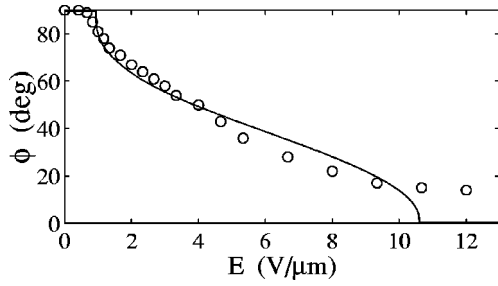


FIG. 3. The azimuthal angle ϕ as a function of the applied field for the field-induced orientational transition depicted in Figs. 1 and 2 (circles, experimental data; solid line, theoretical simulation). The material parameters are the same as in Fig. 2 and the temperature is $T \sim 50$ °C.

ing an electric field across the cell. The schematic sketches in Figs. 1(b) and 1(c) show the observed effect of the field on liquid-crystal orientation at constant temperature ($T \sim 50$ °C). The arrows in Figs. 1(b) and 1(c) indicate the reorientation occurring on increasing the field. The driving force of the phenomenon is the dielectric coupling between the electric field and the nematic molecules which results in an increase of the tilt from the surface (decreased polar angle) and since there is a coupling between the polar and azimuthal angle [3,5,16] also the azimuthal angle changes. If we perform our study in a large temperature range, as depicted in Fig. 2, we see that the temperature-induced reorientation starts at approximately the same temperature independently if the voltage is applied or not, while the maximum reorientation is significantly lower with the voltage applied than without. These maximum positions (shown for 0 and 6 V in Fig. 2) for different applied fields are depicted in Fig. 3 (the circles represent the experimental values whereas the line is given by the theory that will be presented below). From the figure it is clear that the amount of the maximum temperature-induced reorientation decreases for high fields. In this sense the effect of the field is the same as decreasing the temperature; the nematic director approaches the initial orientation given by the evaporation angle and found at low temperatures. The reorientation shown in Fig. 3 for different applied fields was measured at a constant temperature which gives maximum reorientation ($T \sim 50$ °C, see also Fig. 2). In this electrically induced transition the nematic orientation is initially perpendicular to the evaporation plane ($\phi = 90^\circ$) and moves “upwards” on the plane as the field is increased. The measurements presented in this paper were obtained using an ac voltage of $f = 100$ Hz.

The effect depicted in Fig. 3 could itself be used as an electro-optic effect [17]. The switching is in the ms range and has a large component in the plane of the sample even though the field is applied perpendicular to the boundaries. This and a few other possibilities will be discussed further in Sec. IV.

III. THEORY

A. Elastic theory and 3D \rightarrow 2D reduction of the problem

Let us consider a nematic sample of the usual slab shape, limited by two plane-parallel identical surfaces. Let the thickness of the sample be d and the average molecular ori-

entation \vec{n} depend only on the z coordinate, which is normal to the walls at $z = \pm d/2$. The nematic director \vec{n} is defined by means of the polar (θ) and azimuthal (ϕ) angles, shown in Figs. 1(b) and 1(c), as follows:

$$\vec{n} = (\sin \theta \cos \phi, \sin \theta \sin \phi, \cos \theta). \quad (1)$$

The polar angle θ is the angle formed by \vec{n} with the geometrical normal to the substrate, whereas the azimuthal angle ϕ is measured with respect to the projection of the SiO_x evaporation direction on the plane of the substrate. Here, we want to analyze the influence of an applied electric field $\vec{E} = E\vec{k}$, where \vec{k} is a unit vector parallel to the z axis, on the nematic orientation. We assume weak anchoring conditions on the two bounding plates. In this framework the total energy per unit surface of the sample, in the one constant approximation, is given by [18]

$$F = \int_{-d/2}^{d/2} \frac{1}{2} k \left\{ \theta'^2 + \sin^2 \theta \phi'^2 \pm \frac{1}{\xi^2} \sin^2 \theta \right\} dz + 2F_s, \quad (2)$$

according to the sign of the dielectric anisotropy of the nematic liquid crystal (the sign $+$ holds for $\epsilon_a > 0$, and $-$ holds for $\epsilon_a < 0$). In Eq. (2), k is the nematic elastic constant, F_s is the anisotropic part of the surface energy on the substrates at $z = \pm d/2$ [19], and ξ is the electric coherence length [18] defined by

$$\frac{1}{\xi^2} = \frac{|\epsilon_a| E^2}{k}. \quad (3)$$

The value of ξ gives an idea of the length over which the orienting effect of the electric field on the director overcomes the orienting effects of the walls. In Eq. (3), $\epsilon_a = \epsilon_{\parallel} - \epsilon_{\perp}$ is the dielectric anisotropy of the nematic liquid crystal with respect to \vec{E} , where \parallel (parallel) and \perp (perpendicular) refer to the nematic director \vec{n} .

The actual values of $\theta(z)$ and $\phi(z)$ are the ones minimizing F given by Eq. (2). Standard calculations [20] give for the bulk the differential equations

$$\theta'' - \frac{1}{2} \sin(2\theta) \left(\phi'^2 \pm \frac{1}{\xi^2} \right) = 0 \quad (4)$$

and

$$\frac{d}{dz} (\sin^2 \theta \phi') = 0, \quad (5)$$

stating that the bulk density of torque vanishes in the equilibrium state. For the boundary conditions one obtains

$$-k \theta' + \frac{\partial F_s}{\partial \theta_s} = 0, \quad z = -d/2, \quad (6)$$

$$-k \sin^2 \theta \phi' + \frac{\partial F_s}{\partial \phi_s} = 0, \quad z = -d/2, \quad (7)$$

where $\theta_s = \theta(\pm d/2)$ and $\phi_s = \phi(\pm d/2)$. Equations (6) and (7) state that the bulk torques transmitted to the surface are

balanced by the surface torques. We note that $\phi' = 0$, i.e., $\phi = \text{const}$, is a solution of Eq. (5). The constant value of $\phi = \phi_s$ is then given by, as it follows from the boundary condition (7),

$$\frac{\partial F_s}{\partial \phi_s} = 0. \quad (8)$$

Let us limit our analysis to the case in which $\phi = \phi_s$, which means that there is no twist in the sample. In this situation Eq. (4) becomes

$$\theta'' = \pm \frac{1}{2\xi^2} \sin(2\theta). \quad (9)$$

From this equation we obtain

$$\theta'^2 = \pm \frac{1}{\xi^2} (\sin^2 \theta - \sin^2 \theta_0), \quad (10)$$

where $\theta_0 = \theta(0)$. Trivial calculations give [21]

$$\int_{\theta_s}^{\theta_0} \frac{d\theta}{\sqrt{\pm(\sin^2 \theta - \sin^2 \theta_0)}} = \frac{d}{2\xi}, \quad (11)$$

from which it is possible to evaluate $\theta_0 = \theta_0(\theta_s; \xi)$. In this case the boundary condition (6) becomes

$$\frac{k}{\xi} \sqrt{\pm(\sin^2 \theta_s - \sin^2 \theta_0)} + \frac{\partial F_s}{\partial \theta_s} = 0. \quad (12)$$

We consider first a sample submitted to an external electric field much larger than the critical field for the Fredericks transition, which is given by [22]

$$E_c = \frac{\pi}{d} \sqrt{\frac{k}{|\epsilon_a|}}. \quad (13)$$

For usual nematic liquid crystals the critical voltage $V_c = E_c d = \pi \sqrt{k/|\epsilon_a|}$ is of the order of a few volts, or smaller. In this case [22] $\theta_0 \rightarrow 0$ if $\epsilon_a > 0$, and $\theta_0 \rightarrow \pi/2$ if $\epsilon_a < 0$, and the boundary condition (12) can be rewritten as

$$\begin{aligned} \frac{k}{\xi} \sin \theta_s + \frac{\partial F_s}{\partial \theta_s} &= 0 \quad \text{for } \epsilon_a > 0, \\ \frac{k}{\xi} \cos \theta_s - \frac{\partial F_s}{\partial \theta_s} &= 0 \quad \text{for } \epsilon_a < 0, \end{aligned} \quad (14)$$

according to the sign of the dielectric anisotropy. These equations show that in the considered limit, the presence of the distorting electric field can be taken into account by changing the anisotropic part of the surface energy F_s to an ‘‘effective’’ surface anchoring energy defined by

$$\begin{aligned} \mathcal{F}_s^{\text{eff}}(\theta_s, \phi_s) &= F_s(\theta_s, \phi_s) - \frac{k}{\xi} \cos \theta_s \quad \text{for } \epsilon_a > 0, \\ \mathcal{F}_s^{\text{eff}}(\theta_s, \phi_s) &= F_s(\theta_s, \phi_s) - \frac{k}{\xi} \sin \theta_s \quad \text{for } \epsilon_a < 0. \end{aligned} \quad (15)$$

In the following we will assume $\epsilon_a > 0$ and that F_s can be approximated by a simple expression derived from a Landau–de Gennes power series expansion [16,23,24],

$$F_s(\theta_s, \phi_s) = \frac{1}{2} A p^2 + \frac{1}{4} B p^4 + \frac{1}{2} a q^2 + \frac{1}{4} b q^4 + \frac{1}{2} c p^2 q^2, \quad (16)$$

where A , B , a , b , and c are phenomenological parameters which can be temperature dependent, and

$$p = \cos \theta_s \quad \text{and} \quad q = \sin \theta_s \sin \phi_s. \quad (17)$$

It follows that the effective surface energy, in the limit of large fields, is given by

$$\begin{aligned} \mathcal{F}_s^{\text{eff}}(\theta_s, \phi_s) &= \frac{1}{2} A p^2 + \frac{1}{4} B p^4 + \frac{1}{2} a q^2 \\ &+ \frac{1}{4} b q^4 + \frac{1}{2} c p^2 q^2 - \frac{k}{\xi} p. \end{aligned} \quad (18)$$

In the limit of large electric fields the stable states can thus be deduced by minimizing $\mathcal{F}_s^{\text{eff}}$ with respect to ϕ_s and θ_s .

B. Nematic orientation induced by large electric fields

The actual orientation of the nematic at the surface is found by means of Eq. (8) and Eq. (14), which we rewrite, in terms of $\mathcal{F}_s^{\text{eff}}$, as

$$\frac{\partial \mathcal{F}_s^{\text{eff}}}{\partial \phi_s} = \frac{\partial \mathcal{F}_s^{\text{eff}}}{\partial \theta_s} = 0. \quad (19)$$

By taking into account Eq. (16) and Eq. (17) we have

$$\frac{\partial \mathcal{F}_s^{\text{eff}}}{\partial \phi_s} = \frac{\partial \mathcal{F}_s^{\text{eff}}}{\partial p} \frac{\partial p}{\partial \phi_s} + \frac{\partial \mathcal{F}_s^{\text{eff}}}{\partial q} \frac{\partial q}{\partial \phi_s} = \frac{\partial \mathcal{F}_s^{\text{eff}}}{\partial q} \frac{\partial q}{\partial \phi_s} = 0, \quad (20)$$

because p is independent of ϕ_s . Equation (20) is equivalent to

$$\frac{\partial \mathcal{F}_s^{\text{eff}}}{\partial \phi_s} = \frac{\partial \mathcal{F}_s^{\text{eff}}}{\partial q} \sin \theta_s \cos \phi_s = 0, \quad (21)$$

as it follows from the definition of q . Further, aimed to explain the above experimental data, we limit our analysis to the tilted state, where θ_s and ϕ_s differ from 0 and $\pi/2$. Since we are interested in the field dependence of the tilted orientation, we deduce from Eq. (21) that

$$\frac{\partial \mathcal{F}_s^{\text{eff}}}{\partial \phi_s} = 0 \quad \text{implies} \quad \frac{\partial \mathcal{F}_s^{\text{eff}}}{\partial q} = 0. \quad (22)$$

Hence, the boundary condition Eq. (8) is equivalent to

$$a + c \cos^2 \theta_s + b \sin^2 \theta_s \sin^2 \phi_s = 0 \quad (23)$$

in the tilted state. We have furthermore

$$\frac{\partial \mathcal{F}_s^{\text{eff}}}{\partial \theta_s} = \frac{\partial \mathcal{F}_s^{\text{eff}}}{\partial p} \frac{\partial p}{\partial \theta_s} + \frac{\partial \mathcal{F}_s^{\text{eff}}}{\partial q} \frac{\partial q}{\partial \theta_s} = 0, \quad (24)$$

which, by taking into account Eq. (22), reads

$$\frac{\partial \mathcal{F}_s^{\text{eff}}}{\partial \theta_s} = \frac{\partial \mathcal{F}_s^{\text{eff}}}{\partial p} \frac{\partial p}{\partial \theta_s} = 0. \quad (25)$$

In the tilted state, Eq. (25) is equivalent to

$$(A + B \cos^2 \theta_s + c \sin^2 \theta_s \sin^2 \phi_s) \cos \theta_s - \frac{k}{\xi} = 0. \quad (26)$$

From Eq. (23) one deduces

$$\sin^2 \theta_s \sin^2 \phi_s = -\frac{a + c \cos^2 \theta_s}{b}. \quad (27)$$

By substituting Eq. (27) into Eq. (26) one has

$$\left(\frac{Ab - ac}{b} + \frac{Bb - c^2}{b} \cos^2 \theta_s \right) \cos \theta_s - \frac{k}{\xi} = 0. \quad (28)$$

If the electric coherence length ξ , given by Eq. (3), is expressed in terms of the critical field E_c , defined in Eq. (13) by means of

$$\frac{1}{\xi} = \frac{\pi E}{d E_c}, \quad (29)$$

then Eq. (28) is of the type

$$(\nu + \eta \cos^2 \theta_s) \cos \theta_s = \mathcal{E}, \quad (30)$$

where

$$\nu = \frac{Ab - ac}{b} \frac{d}{k\pi}, \quad \eta = \frac{Bb - c^2}{b} \frac{d}{k\pi}, \quad \mathcal{E} = \frac{E}{E_c}. \quad (31)$$

When the field dependence of $\theta_s = \theta_s(E)$ is obtained from Eq. (30), one deduces from Eq. (27) that

$$\sin \phi_s = \frac{\sqrt{-[(a/b) + (c/b) \cos^2 \theta_s]}}{\sin \theta_s}, \quad (32)$$

which together with Eq. (30) gives the azimuthal angle as a function of the applied field. It should be noted that Eq. (30) is a cubic equation in $\cos \theta_s$. It can be rewritten in the form

$$\cos^3 \theta_s + (\nu/\eta) \cos \theta_s - (\mathcal{E}/\eta) = 0. \quad (33)$$

The quantity

$$D = (\nu/3\eta)^3 + (\mathcal{E}/2\eta)^2, \quad (34)$$

in the limit of large \mathcal{E} , is positive. Consequently, Eq. (33) has only one real solution given by

$$\cos \theta_s = [(\mathcal{E}/2\eta) + \sqrt{D}]^{1/3} + [(\mathcal{E}/2\eta) - \sqrt{D}]^{1/3}. \quad (35)$$

The analysis presented above is valid when the anisotropic part of the surface energy is given by Eq. (16). In this general case, the orientation of the liquid-crystal molecules at the surface can change without any restriction under the action of an external field \vec{E} or for a temperature variation. In the next section we will discuss a simple case in which \vec{n} at the surface is forced to be oriented within a plane.

C. Molecular reorientation in a plane

The boundary condition represented by Eq. (23), which follows from Eq. (8), can be rewritten as

$$(a + b) + (c - b) \cos^2 \theta_s = b \sin^2 \theta_s \cos^2 \phi_s. \quad (36)$$

Focusing on the experiment, we consider the specific case where $a + b = 0$. A discussion of this assumption is given in more detail in Sec. III D. The relation (36) shows that if $a + b = 0$, then the two angles θ_s and ϕ_s are connected by the equation

$$\tan \theta_s \cos \phi_s = e, \quad (37)$$

where

$$e^2 = \frac{c - b}{b}. \quad (38)$$

Hence, if $a + b = 0$, \vec{n} moves on the *plane* defined by Eq. (37), as experimentally observed for other orientational transitions on evaporated SiO_x [3–5,7,16]. For this reason, we will assume in the following that $b = -a$. In this framework and by means of Eq. (37) we obtain that q , defined in Eq. (17), can be expressed in terms of p as

$$q^2 = 1 - (1 + e^2)p^2. \quad (39)$$

Consequently, when the constraint represented by Eq. (37) is taken into account, the anisotropic part of the surface energy F_s , given by Eq. (16), reads

$$F_s(\theta_s, \phi_s) = \frac{1}{4}a + \frac{1}{2}(A + c)p^2 + \frac{1}{4}[B - (a + 2c)(1 + e^2)]p^4, \quad (40)$$

and the effective surface energy is found to be

$$\mathcal{F}_s^{\text{eff}}(\theta_s, \phi_s) = -\frac{k}{\xi}p + \frac{1}{4}a + \frac{1}{2}(A + c)p^2 + \frac{1}{4}[B - (a + 2c)(1 + e^2)]p^4. \quad (41)$$

The polar angle $\theta_s(E)$ is still given by Eq. (30) but the parameters ν and η are instead given by

$$\nu = -(A + c) \frac{d}{k\pi}, \quad \eta = -[B - (a + 2c)(1 + e^2)] \frac{d}{k\pi}. \quad (42)$$

Equation (32) for the azimuthal angle is now reduced to the simple expression

$$\sin \phi_s = \frac{\sqrt{1 - (1 + e^2) \cos^2 \theta_s}}{\sin \theta_s}, \quad (43)$$

which contains the single parameter e , given by Eq. (37) above. Equation (43) has been used to obtain the theoretical plot of the azimuthal angle $\phi(E)$ in Fig. 3.

Here we would like to stress that for $\phi_s \rightarrow 0$ the tilt angle tends to a value Θ such that

$$\tan \Theta = e, \quad (44)$$

as follows from Eq. (37). Consequently, from Eq. (30) we have that the electric field necessary to achieve $\phi = 0$ is given by

$$\mathcal{E}_{\text{sat}} = (\nu + \eta \cos^2 \Theta) \cos \Theta, \quad (45)$$

where, as it follows from Eq. (44), $\cos \Theta = 1/\sqrt{1+e^2}$. The field \mathcal{E}_{sat} is a saturation field, in the sense that for $\mathcal{E} > \mathcal{E}_{\text{sat}}$, the director \vec{n} at the surface does not move any longer, but it remains along the direction defined by $\phi_s = 0$ and $\theta_s = \Theta$. For $\mathcal{E} \rightarrow \mathcal{E}_{\text{sat}}$, $\theta_s \rightarrow \Theta$ and $\phi_s \rightarrow 0$ in two different manners. In fact, if $\theta_s = \Theta - \Delta_s$, then for $\mathcal{E} \rightarrow \mathcal{E}_{\text{sat}}$ we have, in the small-angle approximation, from Eqs. (30) and (45) that

$$\Delta_s = \omega_{\text{sat}} (\mathcal{E}_{\text{sat}} - \mathcal{E}), \quad (46)$$

whereas from Eq. (37), in the same limit one obtains

$$\phi_s = \gamma_{\text{sat}} \sqrt{\mathcal{E}_{\text{sat}} - \mathcal{E}}, \quad (47)$$

where ω_{sat} and γ_{sat} are two field-independent constants.

Equation (46) shows that for $\mathcal{E} \rightarrow \mathcal{E}_{\text{sat}}$, $\Delta_s \rightarrow 0$ and $d\Delta_s/d\mathcal{E}$ tends to a finite quantity. Hence, θ_s does not have a critical behavior for $\mathcal{E} \rightarrow \mathcal{E}_{\text{sat}}$. On the contrary, from Eq. (47) we deduce that in the considered limit of $\mathcal{E} \rightarrow \mathcal{E}_{\text{sat}}$, $\phi_s \rightarrow 0$, but $d\phi_s/d\mathcal{E} \rightarrow \infty$. Consequently, for $\mathcal{E} \rightarrow \mathcal{E}_{\text{sat}}$ the azimuthal angle ϕ_s has a critical behavior, typical of a second-order phase transition.

D. Nematic orientation induced by electric fields near the critical field

The analysis presented above is valid in the limit of large electric fields, for which $E \gg E_c$, and hence $\mathcal{E} \gg 1$. In that limit, for positive dielectric anisotropy, $\theta_0 = \theta(0) \rightarrow 0$. In this section we want to extend the analysis presented in the preceding section to the case in which $\mathcal{E} \sim \mathcal{E}_c$, i.e., for electric fields E close to the critical one E_c . By again supposing that the surface director is forced to lie on the plane defined by Eq. (37), we have that the anisotropic part of the surface energy which is relevant for the problem under consideration is given by Eq. (40). Consequently, for electric fields close to the threshold, the boundary condition represented by Eq. (12) reads

$$\frac{k}{\xi} \sqrt{\sin^2 \theta_s - \sin^2 \theta_0} - \frac{1}{2} \{ (A+c) + [B - (a+2c)(1+e^2)] \cos^2 \theta_s \} \sin(2\theta_s) = 0. \quad (48)$$

This equation shows that the threshold field \mathcal{E}_c is given by [25]

$$\frac{(\pi/2)\mathcal{E}_c}{\cot[(\pi/2)\mathcal{E}_c]} = \frac{d[A+c+B-(a+2c)(1+e^2)]}{2k}. \quad (49)$$

For $\mathcal{E} \leq \mathcal{E}_c$, the stable state is the initial one in which $\theta_s = \pi/2$ and $\phi_s = \pi/2$, which corresponds to a planar alignment. For $\mathcal{E} \geq \mathcal{E}_c$, the initial uniform planar state becomes unstable. By setting $\theta_s = \pi/2 - \chi_s$, one can deduce from Eq. (49) that for $\mathcal{E} \geq \mathcal{E}_c$ the angle χ_s is given by

$$\chi_s = \omega_c (\mathcal{E} - \mathcal{E}_c)^{1/2}, \quad (50)$$

where ω_c is a field-independent constant. A similar analysis, performed by setting $\phi_s = \pi/2 - \psi_s$ and using Eq. (37), shows that in the considered limit the angle ψ_s is given by

$$\psi_s = e\chi_s = \gamma_c (\mathcal{E} - \mathcal{E}_c)^{1/2}. \quad (51)$$

Equations (50) and (51) show that χ_s and ψ_s , and hence also θ_s and ϕ_s , have a critical behavior for $\mathcal{E} \rightarrow \mathcal{E}_c$, typical of second-order phase transitions.

IV. DISCUSSION

The electrically induced transition described in Sec. II and theoretically analyzed in Sec. III is shown in Fig. 3. The experimental data given in Fig. 3 were taken at constant temperature ($T \sim 50^\circ\text{C}$) and when no electric field is applied, the orientation of the molecules is perpendicular to the

SiO_x evaporation plane ($\phi = 90^\circ$). Then, as the field is applied and the field strength increases and reaches a threshold value, the molecules start to reorient. When the field is increased further, the reorientation continues and it can reach almost 80° . The theoretical simulations, represented by the solid line in Fig. 3, were derived from Eqs. (30) and (43). The course of the action is to first find the field dependence of the polar angle θ , which is given as a function of the applied field $\theta(E)$ in Eq. (30), and then to insert it into Eq. (43), which gives the azimuthal angle as a function of the applied field $\phi(E)$. Since the solution described above is valid only for fields larger than the critical one, we had to use Eqs. (50) and (51) to find the threshold in ϕ . The agreement between the experimental points and the theoretical simulations are, for this simple model, satisfying. This is especially apparent when considering that the field dependence of $\phi(E)$ [Eq. (43)] contains only one free parameter. The most severe disagreement between the theoretical curve and the experimental data can be found for ϕ values close to zero. As the orientation approaches the initial orientation it had for low temperatures, the reorientation saturates at a value above zero (remember that increasing the field or decreasing the temperature has the same effect on the orientation). This behavior can be explained in the framework of our theory, however the specific relation $a+b=0$ should be refused [see formulas (36)–(40)]. To avoid cumbersome formulas we do not give here this more complete analysis. Instead of the slow saturation of ϕ presented above, our simple theory gives a critical behavior when ϕ approaches zero. The arti-

ficial saturation field and the dependence of ϕ on E close to this point is given by Eqs. (45) and (47) above. Up to now, no evidence of these theoretical predictions has been found experimentally. Another shortage of our theory is that it is unable to account for a small hysteresis that has been observed [17] (not shown in the figures here).

An important point is the assumption that the director moves on an artificial plane which is slightly tilted with respect to the substrate plane, see Fig. 1(b). In the derivation of the theoretical formulas, this was used as an assumption but it could be turned in another way. Instead, the general equations (30) and (32) can be used to fit the data. Interestingly, it turns out that the best fit is achieved just with the parameters describing the plane given by Eq. (37). This justifies our assumption. Our model also gives a simple intuitive picture of the observed phenomenon. The effect of the electric field is to increase the molecular tilt from the SiO_x surface and since the director is bounded to lie within the plane, also the azimuthal angle changes. This reorientation seems to be similar to the orientational transitions upon changing the evaporation angle and the temperature [3,5,16].

The electrically induced transition can be used as an electro-optic effect, as mentioned in Sec. II. The switching of the liquid-crystal molecules and thus also the optic axis is reasonably fast and has a character similar to the in-plane switching of nematic liquid crystals [26,27]. So far, the temperature interval that can be used for our type of switching is too narrow and too high up in temperature. One possibility to avoid this problem could be to use a nematic material with negative dielectric anisotropy. In that case the electrically induced reorientation should start from small azimuthal angles ($\phi \sim 0$) and increase as the field is increased. The advantage would be that the orientation is close to the azimuthal plane ($\phi = 0$) already at low (room) temperatures. Another advantage would be that the birefringence would not decrease as the field strength is increased. The idea is in fact similar to the reorientation of nematic liquid crystals in hybrid cells with gratings which recently has been reported [28]. However, we have not yet been able to optimize the conditions (evaporation angle, SiO_x thickness, etc.) for liquid-crystal materials with high negative dielectric anisotropy. Another possible application of the phenomenon could be in devices utilizing the combination of thermal effects and electro-optic response. The possibility to control the nematic

orientation by means of a strong laser has already been demonstrated [6].

In our analysis, the effect of the electric field on the order parameter has been neglected. This is because, as shown in [29], only very large electric fields (of the order of $50 \text{ V}/\mu\text{m}$) are able to induce a detectable variation of nematic scalar order parameter.

V. CONCLUSIONS

We have analyzed an electrically induced orientational transition in a nematic liquid crystal aligned by obliquely evaporated SiO_x in the range of twofold-degenerate alignment. The driving force of the phenomenon is the dielectric coupling between the molecules and the applied electric field. The switching of the nematic orientation occurs with a large component in the plane of the sample even though the field is applied normally to the surfaces of the substrates. Our theoretical model fits the experimental data fairly well, except when the orientation approaches the position close to the SiO_x evaporation plane. The theory correctly describes a threshold phenomenon at low electric fields and the corresponding critical behavior for the polar and azimuthal angles. The simulations give support for the idea that the reorientation process at the surfaces occurs on an artificial plane which is tilted at about 20° with respect to the substrate plane. The results of our theory can be considered as a general property of nematic liquid crystal in a geometry similar to the one presented here, since the theory is only based on symmetry arguments and on the elastic theory of the nematic phase. Some device implementations of the reported phenomenon are feasible.

ACKNOWLEDGMENTS

This work has been partially supported by the European Union in the frame of the INCO-Copernicus Project ‘‘Novel Techniques and Models for the Surface Treatments of Liquid Crystals with Optical Applications’’ and the SALC Project ‘‘Surface Properties from Basics to Applications in Liquid Crystals.’’ A.K.Z. was also supported by the Politecnico di Torino in the frame of the scientific collaboration between the Politecnico di Torino and the Russian Academy of Sciences.

-
- [1] G. Barbero, Z. Gabbasova, and M. A. Osipov, *J. Phys. II* **1**, 691 (1991).
 - [2] G. Barbero and G. Durand, *Phys. Rev. E* **48**, 1942 (1993).
 - [3] M. Monkade, M. Boix, and G. Durand, *Europhys. Lett.* **5**, 697 (1988).
 - [4] B. Jerome, M. Boix, and P. Pieranski, *Europhys. Lett.* **5**, 693 (1988).
 - [5] P. Jägemalm and L. Komitov, *Liq. Cryst.* **23**, 1 (1997).
 - [6] P. Jägemalm, D. S. Herman, L. Komitov, and F. Simoni, *Liq. Cryst.* **24**, 335 (1998).
 - [7] R. Barberi, M. Giocondo, M. Iovane, I. Dozov, and E. Polosat, *Liq. Cryst.* **25**, 23 (1998).
 - [8] R. Barberi and G. Durand, *Appl. Phys. Lett.* **58**, 2907 (1991).
 - [9] R. Barberi, M. Giocondo, and G. Durand, *Appl. Phys. Lett.* **60**, 1085 (1992).
 - [10] J. L. Janning, *Appl. Phys. Lett.* **21**, 173 (1972).
 - [11] L. A. Goodman, J. T. Meginn, C. H. Anderson, and F. Digeronimo, *IEEE Trans. Electron Devices* **24**, 795 (1977).
 - [12] M. Monkade, Ph. Martinot-Lagarde, G. Durand, and C. Granjean, *J. Phys. II* **7**, 1577 (1997).
 - [13] E. Guyon, P. Pieranski, and M. Boix, *Lett. Appl. Eng. Sci.* **1**, 19 (1973).
 - [14] W. Urbach, P. Pieranski, and M. Boix, *Appl. Phys. Lett.* **25**, 19 (1974).
 - [15] M. Nobili and G. Durand, *Europhys. Lett.* **25**, 527 (1994).

- [16] P. Jägemalm, G. Barbero, L. Komitov, and A. Strigazzi, *Phys. Lett. A* **235**, 621 (1997).
- [17] P. Jägemalm, L. Komitov, and G. Barbero, *Appl. Phys. Lett.* **73**, 1616 (1998).
- [18] P. G. de Gennes, *The Physics of Liquid Crystals* (Clarendon Press, Oxford, 1974).
- [19] S. Faetti, *The Physics of Liquid Crystalline Materials*, edited by I. C. Khoo and F. Simoni (Gordon and Breach, Philadelphia, 1993).
- [20] L. Elsgolts, *Differential Equations and the Calculus of Variations* (MIR, Moscow, 1985).
- [21] S. Chandrasekar, *Liquid Crystals* (Cambridge University Press, Cambridge, 1977).
- [22] E. B. Priestley, P. J. Wojtowicz, and Ping Sheng, *Introduction to Liquid Crystals* (Plenum Press, New York, 1974).
- [23] B. Jerome and P. Pieranski, *J. Phys. (France)* **49**, 1601 (1988).
- [24] A. L. Alexe-Ionescu, G. Barbero, Z. Gabbasova, G. Sayko, and A. K. Zvezdin, *Phys. Rev. E* **49**, 5354 (1994).
- [25] R. Barberi and G. Barbero, *The Physics of Liquid Crystalline Materials*, edited by I. C. Khoo and F. Simoni (Gordon and Breach, Philadelphia, 1993).
- [26] R. Kiefer, B. Weber, F. Windscheid, and G. Baur, in *Proceedings of the Twelfth International Display Research Conference—Japan Display '92, Hiroshima, 1992*, edited by S. Kobayashi, M. Fukushima, and T. Uchida (Institute of Television Engineers of Japan and Society for Information Display, 1992), p. 547.
- [27] M. Oh-e, M. Ohta, S. Aratani, and K. Kondo, in *Proceedings of the Fifteenth Annual Display Research Conference—Asia Display '95, Hamamatsu, 1995*, edited by H. Uchiike, H. Hori, and S. Mikoshiba (Institute of Television Engineers of Japan and Society for Information Display, 1995), p. 577.
- [28] Presented by G. P. Bryan-Brown *et al.* at the SALC meeting (see Acknowledgments) in Moena, Italy, 1998 (unpublished).
- [29] I. Lelidis and G. Durand, *Phys. Rev. E* **48**, 3822 (1994).